THE SCALEX CAMPAIGN

Scale-Crossing Land Surface and Boundary Layer Processes in the TERENO-preAlpine Observatory

B. Wolf, C. Chwala, B. Fersch, J. Garvelmann, W. Junkermann, M. J. Zeeman, A. Angerer, B. Adler, C. Beck, C. Brosy, P. Brugger, S. Emeis, M. Dannenmann, F. De Roo, E. Diaz-Pines, E. Haas, M. Hagen, I. Hajnsek, J. Jacobeit, T. Jagdhuber, N. Kalthoff, R. Kiese, H. Kunstmann, O. Kosak, R. Krieg, C. Malchow, M. Mauder, R. Merz, C. Notarnicola, A. Philipp, W. Reif, S. Reineke, T. Rödiger, N. Ruehr, K. Schäfer, M. Schrön, A. Senatore, H. Shupe, I. Völksch, C. Wanninger, S. Zacharias, and H. P. Schmid

Augmenting long-term ecosystem–atmosphere observations with multidisciplinary intensive campaigns aims to close gaps in spatial and temporal scales of observation for energy and biogeochemical cycling and stimulate collaborative research.

ScaleX is an intensive interdisciplinary observation campaign in a region of complex topography and land-use/land-cover variations in southern Germany. It explores the question of how well measured and modeled components of biogeochemical and biophysical cycles match at the interfaces of soils, vegetation, and the atmosphere, and across various spatial and temporal scales. This type of lead question is not new: scale integration in observation and modeling for land surface–atmosphere exchange processes was one of the principal motivations for past large-scale field programs, such as the First International Satellite Land Surface Climatology Project (ISLSCP) Field Experiment (FIFE), which was conducted in Kansas (Sellers et al. 1988, 1992); the Canadian Boreal Ecosystem–Atmosphere Study (BOREAS; e.g., Hall 1999; Sellers et al. 1995, as well as articles in the same issue); and the Carbon in the Mountains Experiment (CME; e.g., Sun et al. 2010; Desai et al. 2011) to name just three prominent examples. These (and other) field programs have resulted in numerous publications, have spawned research ideas, and

led to new observation and modeling techniques in ecosystem–atmosphere science. Data from these programs have served as valuable benchmarks for model development and measurement intercomparisons, and have contributed significantly to progress in scale integration and the matching of observations and modeling. So why should we endeavor on yet other field campaigns with similar objectives?

This question has many answers. First, despite the progress achieved by past field campaigns, the mismatch between observations of land surface processes and their modeled equivalents is still so large that it constitutes a major source of uncertainty in climate models (e.g., Best et al. 2015). Second, new knowledge in science invariably gives rise to new questions (Firestein 2012). As we learn more about dominant processes and feedback relations, we discover patterns of discrepancy and unexplained deviations at previously disregarded scales that are potentially responsible for long-term trends. Third, progress in instrumentation and data communications allows us to close gaps in the temporal and spatial coverage

of observations that previous field campaigns were limited by. Last, experience shows that whenever scientists from various backgrounds work together, on the same objectives, and on the same field sites, collaboration fosters new ideas and outside-the-box thinking that gives rise to new knowledge (Hall 1999; Goring et al. 2014).

In our view, these points alone justify a new scale-crossing field campaign such as ScaleX. However, in a number of ways ScaleX is different from previous field programs. As presented below, ScaleX is directed at a range of spatial scales that is generally smaller, but with higher measurement and modeling resolution and more complex topography than considered in previous land surface–atmosphere processes campaigns.

Yet the most important novelty of ScaleX probably lies in its infrastructural setting and temporal outlook. The backbone of micrometeorological, hydrological, and ecosystem–atmosphere exchange instrumentation used by ScaleX is formed by the permanent pre-Alpine observatory of the Terrestrial Environmental Observatories network (TERENO-preAlpine; Zacharias et al. 2011), with stations distributed along an elevation gradient in the Prealpine region of Germany (see the section below on the TERENO-preAlpine). The ScaleX campaign builds on this research infrastructure with a multitude of additional instruments and observation platforms (ground-based in situ, remote sensing, and airborne) to enhance spatial and temporal measurement resolutions and to complement the permanent suite of measurements with additional observed variables and processes. The first campaign (ScaleX-2015, June–July 2015) was run by the Division of Atmospheric Environmental Research (IFU) of the Institute of Meteorology and Climate Research (IMK) of the Karlsruhe Institute of Technology (KIT; the institute that operates the backbone infrastructure) in Garmisch-Partenkirchen, Germany, with collaborating partners from the region (see list of coauthor affiliations). The second campaign, ScaleX-2016, took place in June and July 2016 and included a larger number of national and international partners and collaborators (see www.scalex.imk-ifu.kit.edu). Because the TERENO-preAlpine observatory is set to be operated for the next two decades or longer, it will be possible to revisit the same sites periodically in future editions of ScaleX. In our view this long-term continuity is a valuable opportunity to expand the usual narrow temporal constraint of intensive measurement campaigns toward time scales that are important for land-use change, climate change, and ecosystem renewal. The ScaleX concept can likely serve as a model for similar combinations of long-term backbone observatories and periodic intensive campaigns in other permanently operated ecosystem–atmosphere observatories, such as in the AmeriFlux network (Baldocchi 2003; Boden et al. 2013) and the National Ecological Observatory Network (NEON; Kampe et al. 2010) of the United States, or the Integrated Carbon Observation System (ICOS; https://icos-ri.eu) in Europe.

In short, the general idea of ScaleX is to introduce a concept that combines the objectives of long-term ecosystem research with those of intensive campaigns, to expand the scale and resolution of observations, and to stimulate collaborative, interdisciplinary research and synergistic interactions.

AFFILIATIONS: Wolf, Chwala, Fersch, Garvelmann, Junkermann, Zeeman, Brosy, Brugger, Emeis, Dannenmann, De Roo, Diaz-Pines, Haas, Kiese, Malchow, Mauder, Reineke, Ruehr, Schäfer, Shupe, Völksch, and Schmid—Division of Atmospheric Environmental Research (IFU), Institute of Meteorology and Climate Research (IMK), Karlsruhe Institute of Technology, Garmisch-Partenkirchen, Germany; Angerer, Kosak, Reif, and Wanninger—Institute for Software and Systems Engineering, University of Augsburg, Augsburg, Germany; Adler and Kalthoff—Division of Troposphere Research (TRO), Institute of Meteorology and Climate Research (IMK), Karlsruhe Institute of Technology, Karlsruhe, Germany; Beck, Jacobeit, and Philipp—Institute of Geography (IGUA), University of Augsburg, Augsburg, Germany; Hagen—Institute of Atmospheric Physics, German Aerospace Center (DLR), Oberpfaffenhofen, Germany; Hajnsek—Department of Radar Concepts, DLR, Oberpfaffenhofen, Germany, and Institute of Environmental Engineering, ETH Zürich, Zürich, Switzerland; Jagdhuber—Department of Radar Concepts, DLR, Oberpfaffenhofen, Germany; Kunstmann—Division of Atmospheric Environmental Research (IFU), Institute of Meteorology and Climate Research (IMK), Karlsruhe Institute of Technology, Garmisch-Partenkirchen, and Institute of Geography (IGUA), University of Augsburg, Augsburg, Germany; Krieg, Merz, and Rödiger—Department of Catchment Hydrology, Helmholtz-Centre for Environmental Research (UFZ), Halle/Saale, Germany; Notarnicola—Institute for Applied Remote Sensing, European Academy of Bolzano (EURAC), Bolzano, Italy; Schrön and Zacharias—Department Monitoring and Exploration Technologies, Helmholtz-Centre for Environmental Research (UFZ), Leipzig, Germany; Senatore—Department of Civil and Chemical Engineering, University of Calabria, Rende, Cosenza, Italy
CORRESPONDING AUTHOR: Benjamin Wolf, benjamin.wolf@kit.edu

The abstract for this article can be found in this issue, following the table of contents.

The purpose of the present article is to provide some background on the rationale, organization, and specific research goals of ScaleX; to briefly introduce the TERENO-preAlpine observatory with its principal site and the long-term backbone observation program; to give an overview of the instrumentation deployed during ScaleX-2015; and to present examples of derived data products. Last, but most importantly, this article hopes to attract interested research groups as collaborating partners in future campaigns of ScaleX.

BACKGROUND. In the biogeochemical and biophysical cycles that shape our world, terrestrial and aquatic ecosystems are the most important brokers for energy and matter exchanges between the atmosphere, oceans, and continents. They provide natural resources, are mediators of climate change, and contribute to water availability and soil conservation. Terrestrial ecosystems in particular are extremely variable over a wide range of scales both in space and time, and yet they form the most direct foundation for the majority of food production and water and air quality that humanity depends on. Processes, such as the flows of energy, water, oxygen (O), carbon (C), nitrogen (N), and other essential trace substances in and between ecosystems and their environment, indicate the vibrance and variability of ecosystems, and underline the interdependency of supporting, provisioning, and regulating services that ecosystems provide (e.g., Reid et al. 2005).

In terrestrial ecosystems, important exchange fluxes occur at the interfaces of the Earth system compartments—atmosphere, biosphere, pedosphere, and hydrosphere—that each act as reservoirs and sites of transformation in biogeochemical and energy cycling. Given their different nature, chemical and physical transformation and transport processes within these compartments act on vastly different temporal and spatial scales (temporally from fractions of a second for turbulence and biochemical light responses, to decades or longer for climate trends and soil development; spatially from soil microbes to hydrological catchments or landscape units; e.g., Ehleringer and Field 1993), and interactions between them are typically characterized by highly nonlinear feedback dynamics. Thus, no single natural scale of study exists that can adequately represent the manifold interplay of ecosystem–atmosphere processes (e.g., Levin 1992). Scaling errors typically arise from inconsistencies or nonlinear behavior when observations or models at one scale are transferred or aggregated to another, or when model or measurement resolutions filter out temporal or spatial interactions (e.g., Mahrt 1987; Bünzli and Schmid 1998; Schmid and Lloyd 1999). From this perspective, any activity aiming to understand interactions between Earth system compartments requires a scale-integrative observation strategy and needs to go beyond simply assigning aggregated measured values to a larger spatial or temporal domain (Osmond et al. 2004; May 1999; Caldwell et al. 1993).

One pertinent example for which a scale-integrative observation approach is considered to be essential is the observation of the energy balance at the land surface. The turbulent components of the relevant exchange fluxes (i.e., sensible and latent heat fluxes) are commonly determined by the eddy covariance (EC) method. In typical deployments, EC measurements capture turbulent surface–atmosphere interactions on spatial scales of a few hundred meters or less, and over time scales of an hour or less (e.g., Baldocchi 2003). However, microscale atmospheric processes (e.g., Orlanski 1975) can be influenced by circulation patterns at scales of up to several tens of kilometers, persisting for hours [submesoscale to mesoscale; e.g., Emeis (2015)]. This kind of scale interaction is now widely recognized as a principal cause for the so-called energy balance closure problem (Mauder et al. 2010): in most energy balance observations worldwide, the turbulent components are seen to underestimate the sum of their radiative and conductive counterparts by 10%–20% (e.g., Stoy et al. 2013), likely because of unaccounted for submesoscale and mesoscale contributions to sensible and latent heat transport.

Scale-related complications are of particular concern in complex and fragmented landscapes such as mountain regions, where high spatial variability of land use and topography typically entail abrupt changes in available energy, precipitation, soil moisture, vegetation, or soils (Beniston 2006; Poulos et al. 2012). Thus, ecosystem research in complex environments especially demands scale-integrative approaches for observations and modeling.

The ScaleX-2015 campaign was motivated by far-reaching research questions and topics, including 1) how do mesoscale structures in the atmospheric boundary layer (ABL) influence EC-derived surface fluxes, 2) interaction of trace-gas plumes from strong (anthropogenic) point sources with natural background fluxes, 3) development of instrumentation and methods to use unmanned aerial vehicles (UAVs) for ABL characterization of scalars and turbulence, and 4) how do patterns of precipitation relate to soil moisture and runoff over different temporal and spatial scales.
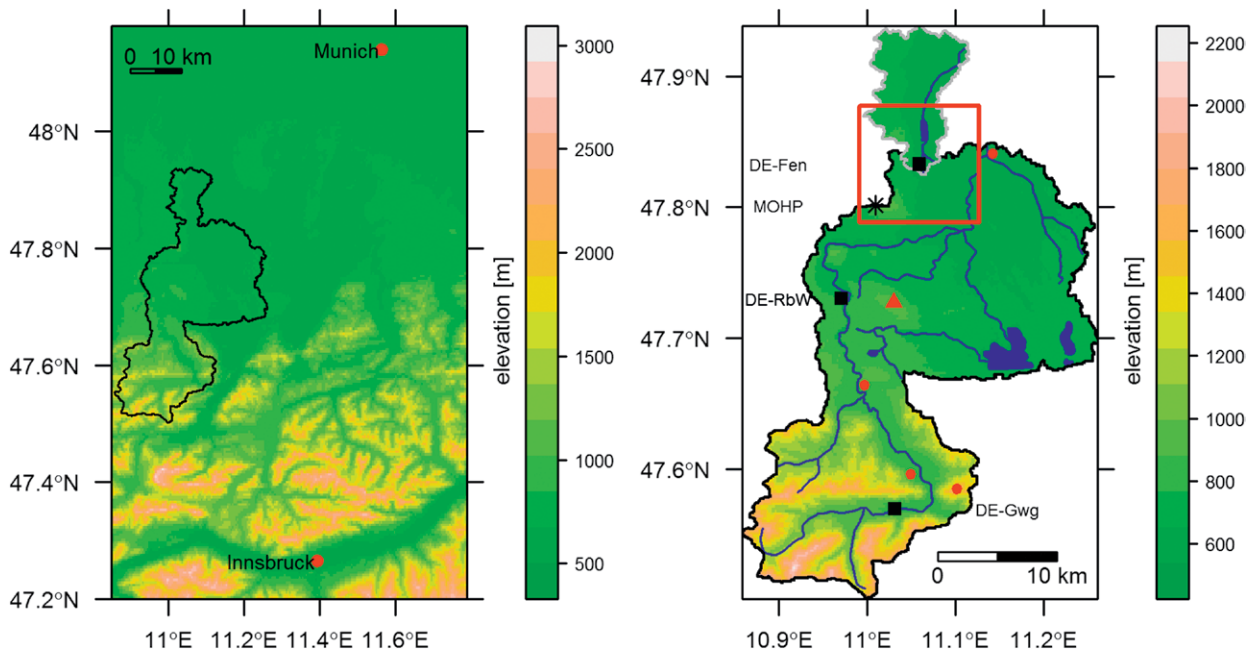
Fig. 1. (left) Location of the TERENO-preAlpine observatory between Innsbruck, Austria, and Munich, Germany. (right) Map of the southern Ammer catchment (black boundary) and the northern Rott catchment (gray boundary), with the three principal sites (black rectangles), precipitation gauges (red dots), X-band rain radar (red triangle), and the meteorological observatory MOHP (black asterisk). See text for details. The red square indicates the ScaleX-2015 study area presented in Fig. 2. Color bars show elevation (m MSL). The maps were produced using Copernicus data and information funded by the European Union–digital elevation model over Europe (EU-DEM) layers (uploaded 8 Oct 2013) and the ATKIS stream network.

Examples of observations in ScaleX-2015 motivated by these questions are presented below in the section dealing with the first data products resulting from this project.

THE TERENO-PREALPINE OBSERVATORY. The Terrestrial Environmental Observatories in Germany form a network of observatories investigating the ecological and climatic impacts of global environmental change on terrestrial systems (Zacharias et al. 2011). The TERENO-preAlpine observatory is located in the Bavarian foothills of the Alps (i.e., the Bavarian Prealps), with elevations from 450 to 2,000 m above mean sea level (MSL), roughly to the west of an axis between Munich, Germany, and Innsbruck, Austria (Fig. 1). At its core is an extensively instrumented site cluster in the catchments of the Ammer (709 km²) and Rott (55 km²) Rivers. With dairy farming as the dominant land use in the valleys of this region, the Prealpine observatory includes the grassland sites Fendt, Rottenbuch, and Graswang (www.europe-fluxdata.eu; station codes are DE-Fen, DE-RbW, and DE-Gwg, respectively) at elevations of 595, 769, and 864 m MSL, respectively (see Fig.1; Zeeman et al. 2017).

The climate change sensitivity of mountain regions, such as the TERENO-preAlpine observatory, is seen to be amplified compared to global averages (Böhm et al. 2001; Smiatek et al. 2009; Calanca 2007), with expected strong consequences in the regional thermal and precipitation regimes, C and N dynamics, and thus nutrient cycling and ecosystem functioning (Mills et al. 2014). To study the impact of climate change on ecosystem functioning and services, and regional circulation and precipitation patterns, the continuously operated backbone infrastructure of the TERENO-preAlpine observatory includes ecosystem–atmosphere flux stations along an elevation gradient, micrometeorology and boundary layer sounding systems, and a hydrometeorological mesoscale network with precipitation-gauge transects and a rain radar (Fig. 1, right). The ScaleX-2015 campaign focused primarily on DE-Fen, which is described in detail in the next section.

THE DE-FEN SITE AND ITS PERMANENT BACKBONE INSTRUMENTATION. DE-Fen is located at the head of a small tributary stream to the Rott River (Fig. 2). The land use at the bottom of this shallow valley is dominated by grassland, sometimes with small patches of cropland, mostly maize. Three dairy farms are located within a distance of less than 1 km to the south and west of the site. To the west, a plateau parallels the valley approximately 100–130 m
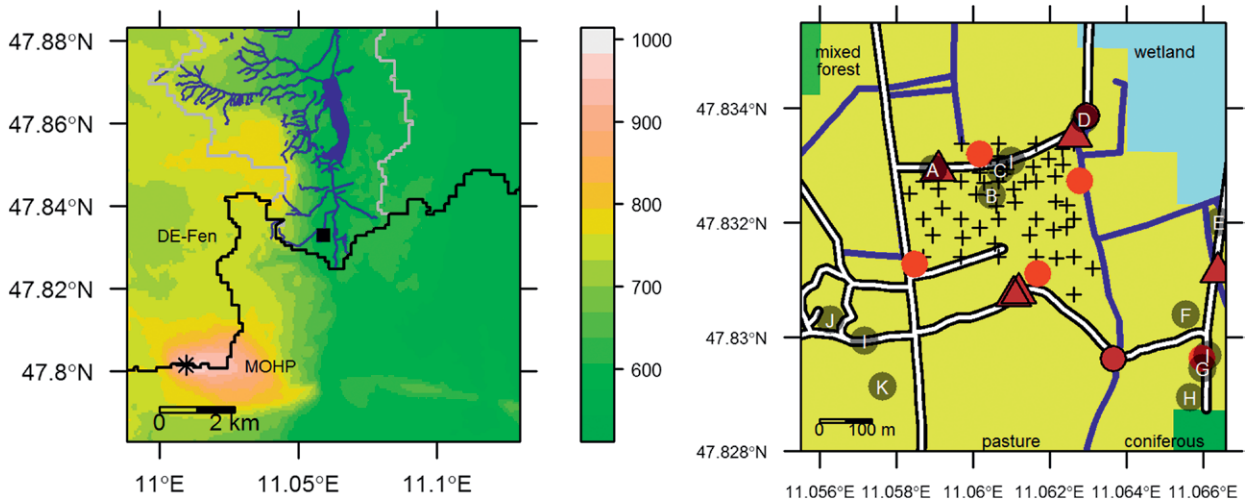
FIG. 2. (left) The ScaleX study area centered around DE-Fen (black square) with topographic features [colors indicate elevation (m MSL)], catchment boundaries (Rott in gray and Ammer in black), and MOHP. Streams and lakes (blue) are shown for the Rott catchment only. (right) Map (~1,000 m × 1,000 m) of land cover (see map), installations, waterways, and roads around DE-Fen with the addition of SoilNetFen nodes (black crosses), precipitation gauges (red dots), groundwater wells (brown triangles), and discharge weirs (brown dots). The letters represent the locations of the remote sensing hub (A), CRNS (B), the EC station (C), an automatic stream-water sampler (D), radio acoustic sounding system (RASS) (E), big chamber (F), the lysimeter cluster (G), the 10-m tower (H), 3D Doppler lidars (I), a nearby farm (J), and an open-path methane analyzer (K). Sonic anemometers at locations A and K, along with a profiler at H, constituted the wind sensor network (see Table 1). Abbreviations are explained in Table 1 and in the text. The maps were produced using the EU-DEM and the Corine Land Cover 2006 raster dataset (European Topic Centre on Spatial Information and Analysis, uploaded 8 Apr 2014, permalink SH04UZP80M) and OpenStreetMap information (www.geofabrik.de, downloaded Jan 2015).

above its floor. The plateau's shoulder is covered predominately with mixed forest. About 5 km southwest of the site the German Weather Service [Deutscher Wetterdienst (DWD)] operates its Meteorological Observatory Hohenpeissenberg (MOHP, 988 m MSL). The northern rim of the Alps lies approximately 30 km to the south.

The permanent backbone instrumentation at DE-Fen includes a micrometeorology station, hydrometeorological installations, and a lysimeter cluster containing the principal local soil types for the measurement of biosphere–atmosphere–hydrosphere exchange processes (specifics of the instrumentation are given in Table 1). The core micrometeorology instrumentation is an EC system (for momentum, CO_2, water vapor, and heat exchange fluxes), a multicomponent surface radiation balance system (including direct and diffuse incoming shortwave radiation), photosynthetically active radiation (PAR), and soil heat flux plates and profiles of soil temperatures and soil moisture, as well as other standard meteorological instruments. This array of in situ instruments (Fig. 2) is augmented by a ceilometer for the determination of the boundary layer height.

To quantify the grassland water balance at high temporal resolution (30 min), the lysimeter cluster (Fig. 2 and Table 1) contains 18 weighable large

(1.0 m², 1.4-m height) grassland–soil monoliths, equipped with soil temperature and moisture sensors. Over each monolith, soil–atmosphere exchange fluxes of CO_2, CH_4, and N_2O are determined through sequential sampling by an automated static chamber system in conjunction with a quantum cascade laser absorption spectrometer.

The heart of the hydrometeorological measurement system at DE-Fen is a wireless sensor network [nicknamed SoilNetFen, following Bogena (2010)] that covers an area of approximately 400 m × 330 m within the footprint of the EC station. SoilNetFen measures soil moisture, soil temperature, and matrix potential every 15 min at 5-, 20-, and 50-cm depths at 55 locations (Fig. 2 and Table 1). A cosmic-ray neutron sensor (CRNS; Zreda et al. 2008) monitors the field-integrated variations of the soil water content. SoilNetFen is augmented by three discharge gauges, five groundwater wells, and one precipitation gauge (Fig. 2 and Table 1).

ADDITIONAL INSTRUMENTATION AND MEASUREMENTS DURING SCALEX. To extend the spatial and temporal scales of observation beyond the range covered by the permanent backbone setup at DE-Fen, the measurement program was

TABLE 1. Permanent and campaign instrumentation at the DE-Fen site, available during ScaleX-2015 (1 Jun–31 Jul). Deployment dates are given for intermittent measurements only. See Figs. 1 and 2 for deployment locations.

Instrument/installation (quantity, if multiple)	Determined quantity	Models and manufacturers (principal components only)
PERMANENT (principal components of TERENO-preAlpine backbone instrumentation at DE-Fen site)		
EC flux station (+ supporting micromet)	CO_2, and latent heat and sensible heat fluxes (supporting micromet, including shortwave and longwave radiation components, PAR, soil heat flux, soil moisture)	CSAT-3,[a] LI-7500[b]
Ceilometer	Aerosol backscatter for ABL height estimation (15-min resolution)	CL51[c]
SoilNetFen network (55 locations, three depths)	Soil volumetric water content (capacitance and frequency domain technology), soil water potential, soil temperature (15-min resolution)	SMT-100[d]
Cosmic-ray neutron sensor	Field-scale topsoil water content	CRS-2000/B[e]
Discharge gauges (2)	River discharge (Thomson V-notch weir)	(by IMK-IFU)[f]
Groundwater wells (5)	Groundwater head	(by IMK-IFU)[f]
Rain gauge	Precipitation	Pluvio[2][g]
X-band radar	Radar reflectivity and precipitation	RAINSCANNER[h]
Lysimeter cluster with static dark chamber system (18)	Groundwater recharge, evapotranspiration, and CO_2, CH_4, and N_2O fluxes	Science Lysimeter,[i] dual-laser trace-gas monitor[j]

complemented during ScaleX-2015 by a combination of additional measurement locations, remote sensing instruments, and airborne platforms (visit www.scalex.imk-ifu.kit.edu for illustrations). Instruments that could not be operated in a continuous mode were integrated by means of intensive observation periods. Specifics of all instruments or installations mentioned in this section are summarized in Table 1.

Boundary layer remote sensing was conducted by three high-resolution scanning Doppler lidar systems for vertical profiles of wind and turbulence (1,000-m maximum), as well as by a radio acoustic sounding system (RASS; Emeis et al. 2009) to determine vertical profiles of wind and temperature (560-m maximum). Resulting data products include the characterization of the turbulence and thermal structure in the boundary layer, as well as the detection of low-level jets. In addition, a ground-based scanning microwave radiometer was operated to obtain integrated water vapor (IWV), liquid water path (LWP), and temperature and humidity profiles.

The remote sensing measurements were complemented by airborne observations. A swarm of UAVs was jointly operated by the IMK-IFU and the Institute for Software and Systems Engineering (ISSE) and the Institute of Geography (IGUA) at the University of Augsburg. The UAVs were flown during different experiments and in coordinated flight patterns (four copters, three fixed-wing aircraft), each equipped with temperature, humidity, and pressure sensors. Because of legal provisions, the maximum ascent of the copters above ground level was limited to 150 m. In addition to the UAVs, the D-MIFU microlight aircraft (see Junkermann 2001; Junkermann et al. 2011; Metzger et al. 2013) was deployed to provide wind, temperature, moisture, turbulent fluxes, and radiation measurements at a larger spatial extent of about 12 km × 12 km around DE-Fen, from 50 m up to 2.5 km above ground level (AGL).

To explore the spatial and temporal variability of precipitation, rain gauges were installed at 5 locations within the SoilNetFen area and at 17 additional locations in the Rott catchment. This gauge network, as well as a Micro Rain Radar (MRR) and two disdrometers, augmented and provided ground truth for the DWD C-band radar at MOHP and the TERENO X-band rain radar (Fig. 1). Furthermore, the chemistry and isotopic composition of precipitation, as well as surface and subsurface water, were tracked by water samples taken both manually and automatically throughout the campaign [using a cavity ring down (CRD) spectrometer; Table 1]. To link the soil moisture measurements at the point and catchment scales, mobile CRNS (TERENO Rover), airborne [synthetic aperture radar (F-SAR)] sensors were used, and linked to satellite-derived data (*RadarSat-2*).

Greenhouse gas (GHG) flux measurements from the lysimeter cluster were complemented by a large

TABLE 1. Continued.

Instrument/installation (quantity, if multiple)	Determined quantity	Models and manufacturers (principal components only)
Additional ScaleX-2015 instrumentation		
Radio acoustic sounding system	Wind and temperature profiles, vertical velocity variance, range of 20–560 m, and 10-min means	482-MHz RASS[k]
Doppler lidar (3)	3D wind and turbulence profiles, range up to 1,000 m in 18-m increments, and 1–3-min means	Streamline[l]
Passive microwave and infra-red radiometer	Temperature and humidity profiles, IWV, and LWP, as well as cloud-base temperature	Humidity and temperature profiler (HATPRO)[m]
Hexacopter	Payload sensors for relative humidity, air temperature, and air pressure; deployment dates of 24, 25, and 30 Jun and 1, 10, 15, 16 20, 21, 23, and 30 Jul	F550 hexacopter[n]
Quadrocopter swarm (3)	Payload sensors for relative humidity, air temperature, and air pressure; deployment dates of 30 Jun, 1 Jul, and 6 Aug	Saphira,[v] Autoquad M4[w]
Fixed-wing UAVs (3)	Payload sensors for relative humidity, air temp, air pressure, and wind; deployment dates of 30 Jun, 1 and 15 Jul, and 6 Aug	(by IGUA)[f]
Microlight aircraft (D-MIFU)	Temperature, dewpoint, and aerosol profiles; turbulent fluxes; and radiation (ultraviolet and infrared); deployment dates of 5, 12, 25, and 26 Jun and 4, 7, 10, 15, 16, and 22 Jul	(for/by IMK-IFU)[f]
Rain gauges (groups of 3)	Precipitation amount, with five groups at DE-Fen and 17 groups within the Rott catchment	Rain Collector[o]
DWD C-band radar	Spatial information on precipitation amount and hydrometeor types	Dual-pole Doppler C-band weather radar (by DWD)[f]
Micro Rain Radar	Vertical profiles of rain rate and drop-size distribution	MRR[k]
Disdrometers (2)	Drop-size distribution, rain rate	Particle size and velocity (Parsivel),[g] laser precipitation monitor [Laser Niederschlags-Monitor (LNM)]p
Cavity ring down spectrometer	Isotopic composition ($^{18}O–H_2O$ and $^2H–H_2O$) of precipitation, groundwater, and streamflow	L1102-i[q]
TERENO Rover	Soil water content, vehicle-based CRNS	CRS-1000[e]
F-SAR	Topsoil water content (one overflight during ScaleX-2015)	L-band SAR (by DLR)[f]
Big chamber	CH_4 soil flux; static chamber principle (dimensions of 10 m × 2.60 m, max height 0.61 m); deployment dates of 9, 16, 25, 26, and 30 Jun and 10, 14, 20, 21, 23, 28, and 30 Jul	(by IMK-IFU)[f]
Trace-gas analyzer	CH_4 and H_2O concentrations	Fast Methane Analyzer[r]
Wind sensor network (three locations)	Wind and turbulence (profile at 1,[s] 5,[s] and 10[a] m, location H in Fig. 2; two stations[s,t] at 3-m height, locations A and K in Fig. 2)	CSAT-3,[a] WindSonic,[s] 81000[t]
CRD spectrometer	CH_4, N_2O, and CO_2 concentrations	G2508[q]
Open-path methane analyzer	Line-averaged methane mixing ratios	Gas Finder 2[u]

Manufacturers: [a] Campbell Scientific, Logan, UT; [b] LI-COR, Lincoln, NE; [c] Vaisala, Helsinki, Finland; [d] TRUEBNER Instruments, Neustadt, Germany; [e] Hydroinnova LLC, Albuquerque, NM; [f] In house or custom built; [g] OTT Hydromet, Kempten, Germany; [h] Selex ES GmbH, Neuss, Germany; [i] UMS, Munich, Germany; [j] Aerodyne Research, Billerica, MA; [k] METEK GmbH, Elmshorn, Germany; [l] Halo Photonics, Worcestershire, United Kingdom; [m] Radiometer Physics GmbH, Meckenheim, Germany; [n] DJI, Beijing, China; [o] Davis Instruments, Hayward, CA; [p] Thies Clima, Göttingen, Germany; [q] Picarro Inc., Santa Clara, CA; [r] Los Gatos Research, San Jose, CA; [s] Gill Instruments, Lymington, United Kingdom; [t] R. M. Young, Traverse City, MI; [u] Boreal Laser Inc., Edmonton, AB, Canada; [v] Rosewhite Multicopter, Mauerstetten, Germany; [w] distributed by iRC-Electronic, Wehringen, Germany.

static chamber [Schäfer et al. (2012), in conjunction with a trace-gas analyzer] for CH_4 flux measurements on a patch of grassland that is frequently flooded, as well as by atmospheric CH_4 concentration measurements. To evaluate the regional CH_4 sink or source strength, profiles of atmospheric CH_4 concentrations (using a CRD) were determined on a tower at heights of 1, 5, and 10 m above ground, and upwind and downwind of a dairy farm (using an open-path methane analyzer; range of ~100 m), along with wind speed and direction (wind sensor network).

SOME FIRST DATA PRODUCTS. The activities in ScaleX-2015 were organized along the overarching research questions of land surface–atmosphere interactions in the atmospheric boundary layer discussed earlier (see the background section). Here, a selection of first data products is presented, to illustrate the range of intensive observations conducted during the ScaleX campaigns.

High-resolution ABL motion structure by a lidar cluster. Standard observations of biosphere–atmosphere exchange (e.g., using the EC method) assume horizontal homogeneity of the turbulence structure and generally ignore the contributions of ABL-scale or mesoscale motions on exchange fluxes. In fragmented landscapes with topography and mixed land use, secondary circulations can develop that affect the validity of standard exchange observations. To account for the effects of such nonlocal motions on turbulent exchange near the surface is difficult, but their exclusion introduces bias in long-term fluxes (Mahrt 1987, 2010).

In ScaleX-2015 a cluster of three Doppler boundary layer lidars was used in conjunction with a network of sonic anemometers to characterize the motion structure over the entire ABL continuously, and at high temporal and spatial resolutions, over the duration of the campaign. The Doppler lidars (Table 1) recorded three-dimensional wind vectors (u, v, and w) in a vertical scanning profile arrangement that served as a virtual tower up to approximately 1,000 m above the surface (Fig. 3, left).

The observations revealed flow features over a range of time and length scales. Figure 3 (right) illustrates a representative day (1 July 2015). The development of thermally driven activity in the ABL at around 0700 UTC (0800 local standard time) was visible first as a change of wind direction and vertical wind speed, starting at the surface and rising rapidly. Daytime flow was dominated by northerly to easterly wind throughout the boundary layer. In addition, the daytime boundary layer was characterized by typical convective motion features over scales of several minutes and vertical extents of several hundred meters. After sunset, the wind direction shifted to the east and a low-level easterly jet formed around 1900 UTC between 200 and 500 m AGL, but this pattern decayed in magnitude around 2330 UTC as shown by the horizontal wind speed. The nighttime wind direction above 200 m stayed mostly southeasterly to easterly, in contrast to layers below 200 m, which showed low wind speed, but directional shear up to 180°, even below the low-level jet.

On this particular day, more than 82% of the recorded nocturnal half-hourly EC observations of CO_2 and heat exchange were rejected, based on standard quality-control criteria, including stationarity, turbulence characteristics, and signal noise (Mauder et al. 2013). The remaining nocturnal surface flux observations coincided with the presence of the low-level jet after sunset. Between 0900 and 1900 UTC no data were rejected or flagged. This nighttime bias of missing turbulence data underlines the difficulty of obtaining nighttime trace-gas flux and transport information, as discussed in the next section. High-resolution ABL motion data, such as those presented here, are anticipated to be valuable in evaluating, for example, large-eddy simulation (LES) models during efforts to assess typically unresolved nonlocal contributions to surface fluxes.

Variability of methane concentration in the nocturnal boundary layer. Methane (CH_4) is an important GHG of predominantly biogenic origin, with ecosystems acting either as net sources or sinks. Wetlands and water-logged soils emit CH_4 as a result of the activity of methanogenic microbes, while upland and well-aerated soils are usually net sinks for atmospheric CH_4, because of the predominance of CH_4-oxidizing microbes. Although methane sensors fast enough for eddy covariance are available, CH_4 fluctuations often range near the limit of sensitivity, and EC signals tend to be noisy (e.g., Hommeltenberg et al. 2014). A convenient alternative approach to consider is the static chamber method [see Pihlatie et al. (2013) for a review]. This method determines surface exchange fluxes over a well-defined area of ground (commonly < 1 m^2), by measuring the trace-gas accumulation or depletion over a given time, referenced to the chamber volume. Because variability in soils (e.g., moisture and substrate availability) typically ranges down to similar spatial scales as the chamber dimensions, the scaling up from chambers to a scale comparable to an EC flux footprint (e.g., Schmid 2002), or to the
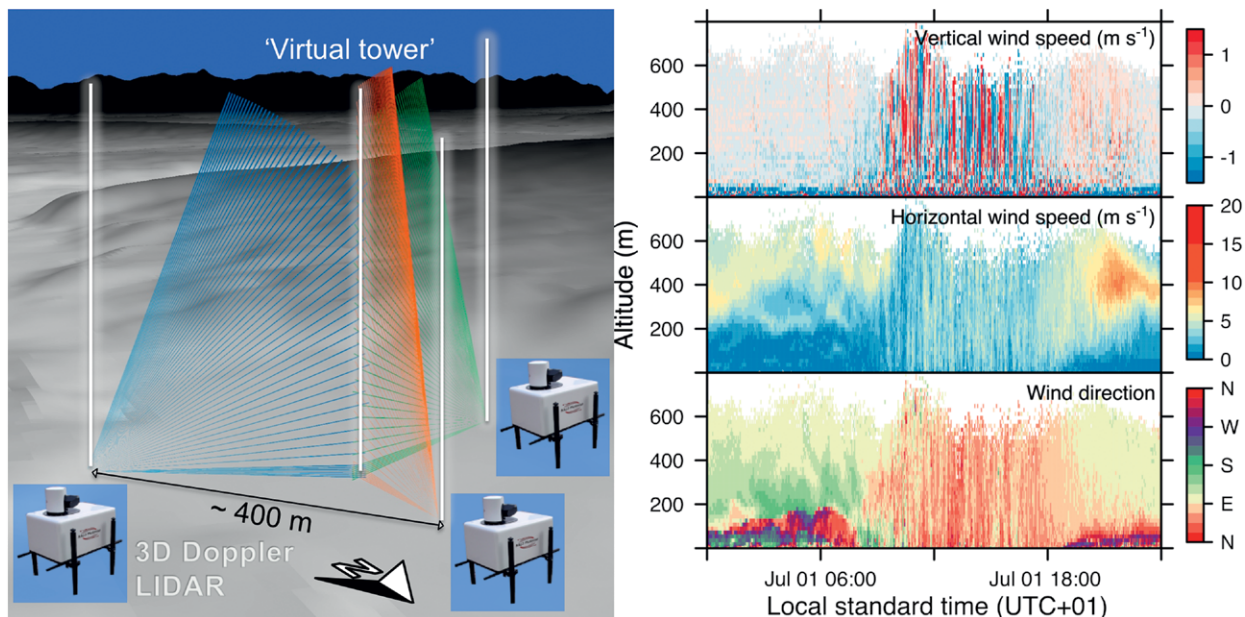
FIG. 3. (left) Schematic illustration of the 3D Doppler lidar setup used to observe a vertical profile of 3D wind vectors (virtual tower). The schematic is superimposed onto a terrain representation of the DE-Fen site. (right) Profiles of vertical and horizontal wind speed and wind direction at the ScaleX virtual tower on 1 Jul 2015. Positive (negative) vertical wind speed indicates upward (downward) motion. Vertical axes represent height above ground level.

resolution at which ecosystem exchange models are commonly run, is a formidable problem (e.g., Pihlatie et al. 2010). An additional confounding problem is posed by larger-scale spatial heterogeneity, for example, in mixed-land-use areas with upland grassland or crops, patches of wetlands, and pastures or barns with methane-producing cattle. Particularly during nighttime stable conditions, plumes of methane-enriched air, for example, can be transported over considerable distances with very little mixing: if such a transient plume increases the local atmospheric CH_4 concentration, the higher CH_4 supply may lead to extra stimulation of the methane-consuming microbes in the soil. The resulting increased uptake rate needs to be quantified and considered when calibrating and validating biogeochemical models designed to simulate the CH_4 exchange based on local soil properties and soil environmental conditions. Transient plumes may also affect nighttime EC measurements of methane: shallow CH_4 plumes may lead to spurious vertical gradients that, in the presence of weak turbulence, introduce a contribution to the EC flux signal that has no linkage to surface sources or sinks in the flux footprint (Finnigan 2004).

Alternately, larger-scale spatially averaged trace-gas fluxes (e.g., at the scale of a model grid cell) can in theory be derived by the boundary layer budget method (Denmead et al. 1996; Emeis 2008), which is an inverse method, where surface fluxes are the residual result of concentration changes and transport terms observed and modeled over a hypothetical box bounded by the height of the ABL.

However, nighttime application of direct or inverse trace-gas flux estimates is a challenge, because very little is known about the spatial and temporal CH_4 variability above the surface in the nocturnal boundary layer (NBL), and observations are difficult and rare. In ScaleX a new approach was explored to assess plumes and gradients of methane in the NBL that may make such observations more accessible in the future. Measurements of atmospheric CH_4 concentrations were performed by pumping ambient air through a sampling tube [Teflon, outer diameter of 1/8 in. (3.2 mm)] to a CRD spectrometer. To extend the nighttime vertical CH_4 profiles to beyond the 10-m tower at DE-Fen (location H in Fig. 2), the end of a sampling line (70-m length) was mounted to an F550 hexacopter and periodically raised to heights of 10, 25, and 50 m AGL. Data are reported as 1-min averages for all heights.

Observations from 21 July 2015 (Fig. 4) showed that atmospheric CH_4 concentrations at all measurement heights increased well above the background concentration (1.9 ppm, determined as the average ABL concentration in well-mixed daytime conditions). The lower sampling heights exhibited strong variations, whereas fluctuations were much reduced above the 10-m tower height. Figure 4 also shows

considerable negative vertical CH_4 concentration gradients, which start to decrease during the second half of the night, indicating slow vertical mixing in the NBL. These findings suggest shallow advection from areas with strong CH_4 sources, because the local grassland soils were sinks for atmospheric CH_4. Concurrent wind directions point to dairy barns nearby as the likely culprit. Observations from other nights confirmed this nighttime advection to be a regular occurrence. The observations also show that the measured values determined by the hexacopter method agree well with the tower measurements at 10 m. They indicate that the method of using UAVs to carry trace-gas intake lines to heights beyond the reach of common instrument masts is promising as a low-cost and flexible way of exploring GHGs or other trace-gas structures in the nocturnal boundary layer.

Use of UAVs and microlight aircraft for three-dimensional boundary layer characterization. One of the biggest challenges for projections of regional climate or ecosystem–atmosphere interactions involves getting the hydrometeorology right (Clark et al. 2015). Without knowledge of how much water is transpired or evaporated across a region, we cannot predict how much CO_2 the plants will assimilate. The amount of water vapor that is transported from one mesoscale model grid cell to another is crucial information for predictions of when and where that water will fall as rain. In complex terrain, it is important to know on which side of a ridge the rain falls, to infer whether vegetation will be water stressed or whether a river

might flood. However, the evaluation of regional-scale hydrometeorological models by observation is challenged by i) the unresolved spatial variability of atmospheric temperature and humidity and ii) a lack of adequate experimental tools to determine the balances of water and heat over model grid cells or model subdomains (Lorenz and Kunstmann 2012). In ScaleX an attempt is made to tackle this problem by combining the hydrometeorological in situ observations of the TERENO-preAlpine observatory with a suite of remote sensing techniques (ground based and airborne), instrumented UAVs, and a microlight aircraft to capture the three-dimensional variability of the atmospheric state variables in the ABL at high resolution. ScaleX-2015 included a proof-of-concept campaign to coordinate the flight patterns of a swarm of UAVs and the microlight aircraft.

The microlight aircraft, D-MIFU, was used to assess 3D distributions of winds, air temperature, dewpoint, latent and sensitive heat fluxes, surface temperature, the radiation balance, and aerosol size distributions. Flights included horizontal tracks as well as vertical "spiral staircase" profiles from about 50 to 2000 m AGL directly above and at the vertices of a 12 km × 12 km rectangle around DE-Fen. At a radius of about 500 m around the DE-Fen EC station, small UAVs were operated to determine the small-scale spatial and temporal variabilities of the thermal structure in the ABL.

Battery-operated UAVs are constrained by flight duration, horizontal distance (~300 m), and maximum ascent, while aircraft are limited by the lowest legally possible flight level (50 m). To capture the thermal structure in the boundary layer over DE-Fen, several vertical profiles of air temperature were determined with the hexacopter, one fixed-wing UAV, and the D-MIFU microlight on 15 July (Fig. 5), each set within about 15–30 min. Though the measurements were not taken at exactly the same time and location, the temperature measurements of all three systems mostly agreed within 0.5°C for the overlapping heights. Therefore, the aerial vehicles complemented each other to obtain a seamless
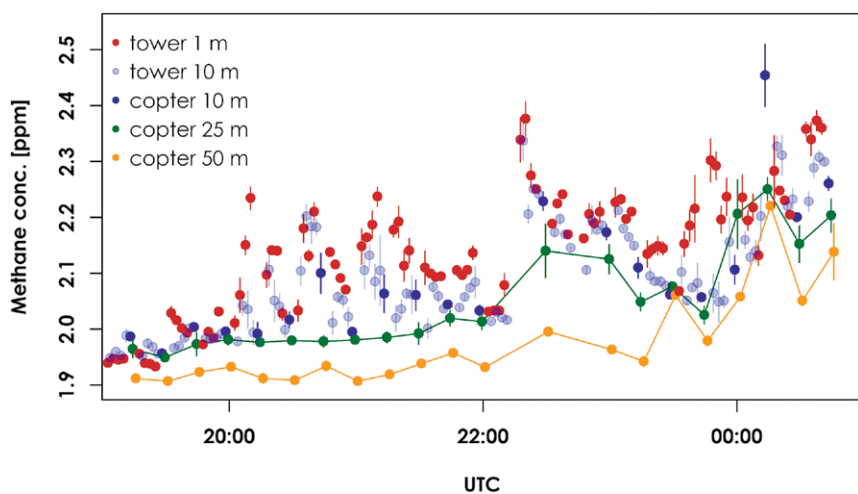

FIG. 4. CH$_4$ concentrations (plus or minus one standard deviation, 1-min means) measured at 1- and 10-m heights on the tower, and by the hexacopter at 10, 25, and 50 m on 21 Jul 2015. To improve legibility of the data at 25 and 50 m, lines were added to connect the measurements at these levels. Local standard time is UTC + 1 h.

representation of the vertical structure from the ground up to the free troposphere.

Together with the use of the hexacopter in trace-gas measurements, these first results are encouraging for the use of lightweight UAVs as an emerging technology in atmospheric boundary layer research. Battery-operated UAVs have no exhaust, and very low heat emissions, and can be programmed to perform complex flight patterns or (for copters) hold a given position even in convectively turbulent conditions. The 2015 campaign also established that a swarm of three copters and three fixed-wing UAVs can be deployed together, to perform complex coordinated sensing patterns in a small boundary layer volume (~300 m wide and high; not shown), for example, to perform in situ measurements at exactly the same time and height but at different locations. The UAVs used here are lightweight (below 2.5 kg) and thus the instrument payload is very limited (currently temperature, humidity, pressure, and wind velocity; see Table 1). With progressive developments in sensor miniaturization, rapid expansion of further research applications of UAVs can be expected in future campaigns.

Soil moisture and precipitation patterns at a range of scales. Precipitation and soil moisture are the fundamental hydrologic quantities required for a more profound understanding of runoff and flood generation, but they are also essential for plant-physiological and biogeochemical processes (Ruehr et al. 2014; Yao et al. 2010; Clough et al. 2004). At the same time,

the measurement of precipitation and soil moisture beyond the point scale is one of the most critical challenges in the hydrological sciences. Therefore, a major focus within the ScaleX campaign concerned the characterization of the spatial and temporal variabilities of rainfall and soil moisture at DE-Fen and within the Rott catchment.

For precipitation, this objective is accomplished using weather radar data and a dense network of rain gauges at 22 locations (Fig. 6) in the Rott River catchment region. The average distance between gauges was 250 m at DE-Fen and 2.5 km in the catchment. To handle random errors in the rain gauge data, each of the 22 locations was equipped with a set of three tipping-bucket rain gauges (Krajewski et al. 2003). With this level of redundancy, spurious outliers and instrumental errors could be identified and the faulty sensor excluded from estimates of precipitation, resulting in quality-controlled and mostly gap-free precipitation time series.

Though the average distance between the rain gauge sites is only 2.5 km, local convective events may remain concealed. To cover the whole target region with high spatial resolution, data from the polarimetric C-band weather radar at MOHP (see Fig. 1) are used. Figure 6 shows an example of the high spatial variability of hourly precipitation during a convective event. While the rain gauge and radar data are in good agreement at the gauge locations, the gauges alone cannot resolve the spatial variability at an hourly scale. The combination of radar and gauges facilitates the validation and adjustment of the radar
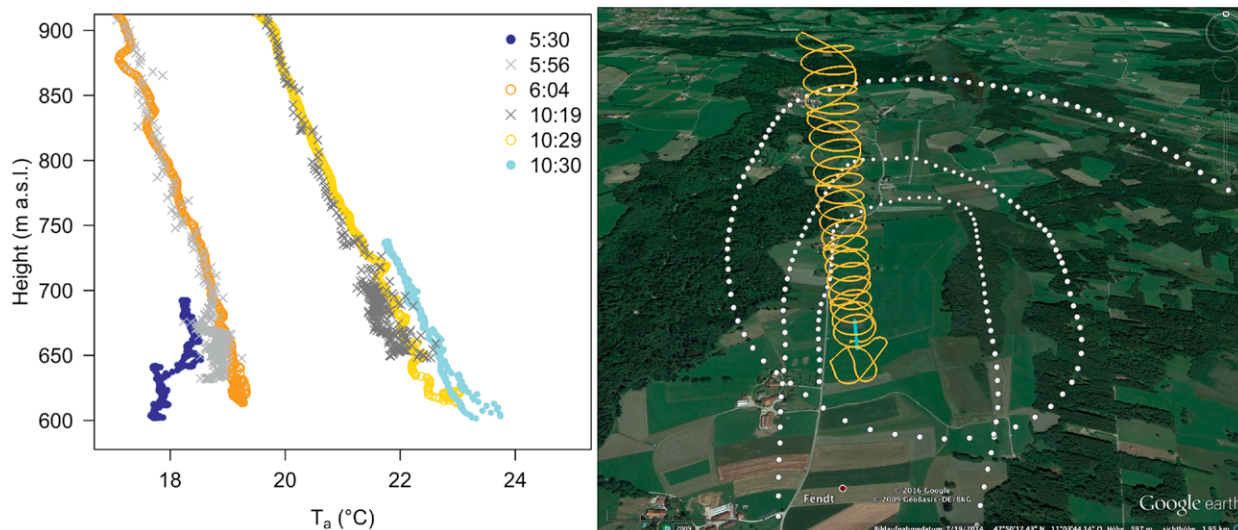

FIG. 5. (left) First 300 m of vertical air temperature (T_a) profiles determined by the hexacopter (shades of blue), fixed-wing UAV (yellow and orange), and D-MIFU (gray) on 15 Jul 2015 (start times given in UTC; local standard time is UTC + 1 h). (right) Profile of flight tracks of D-MIFU (white), fixed-wing UAV (yellow), and hexacopter (blue).
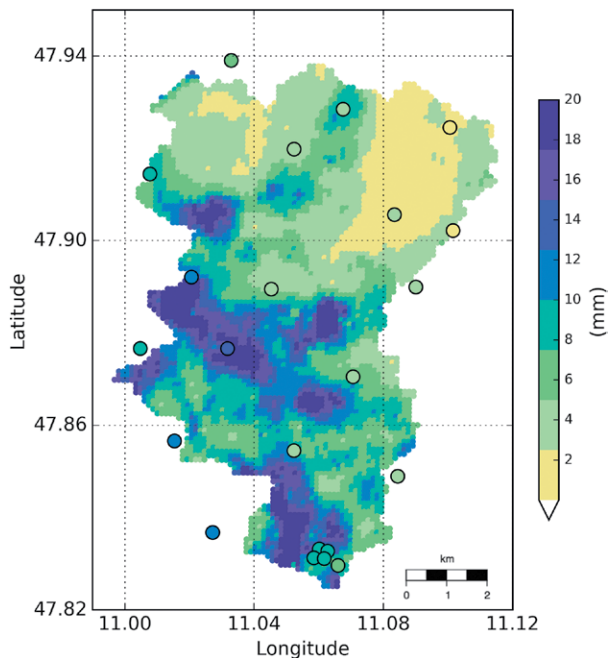
Fig. 6. Example of the high spatial variability of hourly rainfall in the region of the Rott catchment (1600 UTC 27 Jun 2015) recorded by the rain gauge network (color-filled circles) and the DWD C-band weather radar (colored map). The color scale is given in millimeters of hourly precipitation.

field at the gauge locations, as well as corrections to the inherent radar errors. The corrected radar field can then serve as additional high-resolution rainfall information to be used during hydrological modeling.

Soil moisture patterns were identified based on SoilNetFen measurements (Fig. 2). Individual point measurements of soil volumetric water content (VWC) at 5-, 20-, and 50-cm depths were interpolated onto maps for each depth, using a simple inverse-distance weighting scheme (Pebesma 2004). The top and bottom-left panels in Fig. 7 illustrate the resulting moisture fields for 15 July 2015.

ScaleX-2015 included a first comparison of soil moisture distributions determined by the SoilNet-Fen capacitance-based sensors and by the TERENO Rover, a mobile cosmic-ray neutron sensor system mounted on a pickup truck. Introduced by Zreda et al. (2008), CRNS is a relatively new technique for estimating spatially integrated soil moisture, but it is based on theory largely from the 1950s. Primary cosmic rays enter Earth's atmosphere from galactic origins, mainly as protons. Collisions with nuclei in the atmosphere, and later in the soil, generate cascades of neutrons with decreasing levels of energy (secondary cosmic rays). In the words of Zreda et al. (2008, p.1), "soil moisture content on a horizontal

scale of hectometers and at depths of decimeters can be inferred from measurements of low-energy cosmic-ray neutrons that are generated within soil, moderated mainly by hydrogen atoms, and diffused back to the atmosphere. These neutrons are sensitive to water content changes, but largely insensitive to variations in soil chemistry, and their intensity above the surface is inversely correlated with hydrogen content of the soil." However, according to Köhli et al. (2015), the spatial sensitivity of the sensor decreases sharply with distance, and the effective measurement depth depends on the soil type and moisture content, typically ranging from 10 to 40 cm. Stationary CRNS are commonly used for monitoring soil moisture variations over time, while the mobile CRNS TERENO Rover can detect spatial variations along transect paths, filtered by a footprint size on the order of several hundred meters in diameter (Zreda et al. 2008).

The TERENO Rover was repeatedly employed at DE-Fen during ScaleX-2015, as well as along tracks throughout the Rott River catchment. The bottom-right panel in Fig. 7 shows the VWC derived from 127 data points observed by the CRNS along the Rover tracks at DE-Fen (transect velocity of approximately 2 km h^{-1}). Because the southern part of the SoilNetFen area could not be accessed with the vehicle, data are missing from that area. Considering the large footprint of CRNS, the gradient of dry to moist conditions from west to east in SoilNetFen is captured well by the rover, both qualitatively and quantitatively. The "eye" structures of apparent high VWC in the plot are likely artifacts of the basic interpolation method used in these preliminary results.

Runoff-generation mechanisms and storage interactions. Surface water–groundwater interactions are complex (Sophocleous 2002) and crucial for the functioning of riparian ecosystems (Kalbus et al. 2006; Jones and Holmes 1996) and the hyporheic zone (Sophocleous 2002; Kalbus et al. 2006; Jones and Holmes 1996). Because groundwater is usually depleted in heavier stable isotopes compared to surface water bodies (Uhlenbrook et al. 2002; Tetzlaff et al. 2009; Coplen et al. 2000; Hinkle et al. 2001), the stable isotope abundances of oxygen-18 and deuterium in water have been used widely as natural tracers to explore hydrological processes and interactions between surface water and groundwater.

As DE-Fen is located at the bottom of a shallow valley, the hydrodynamic gradient is weak and it can be expected that groundwater–surface water interactions are an important mechanism in the study area. So, not
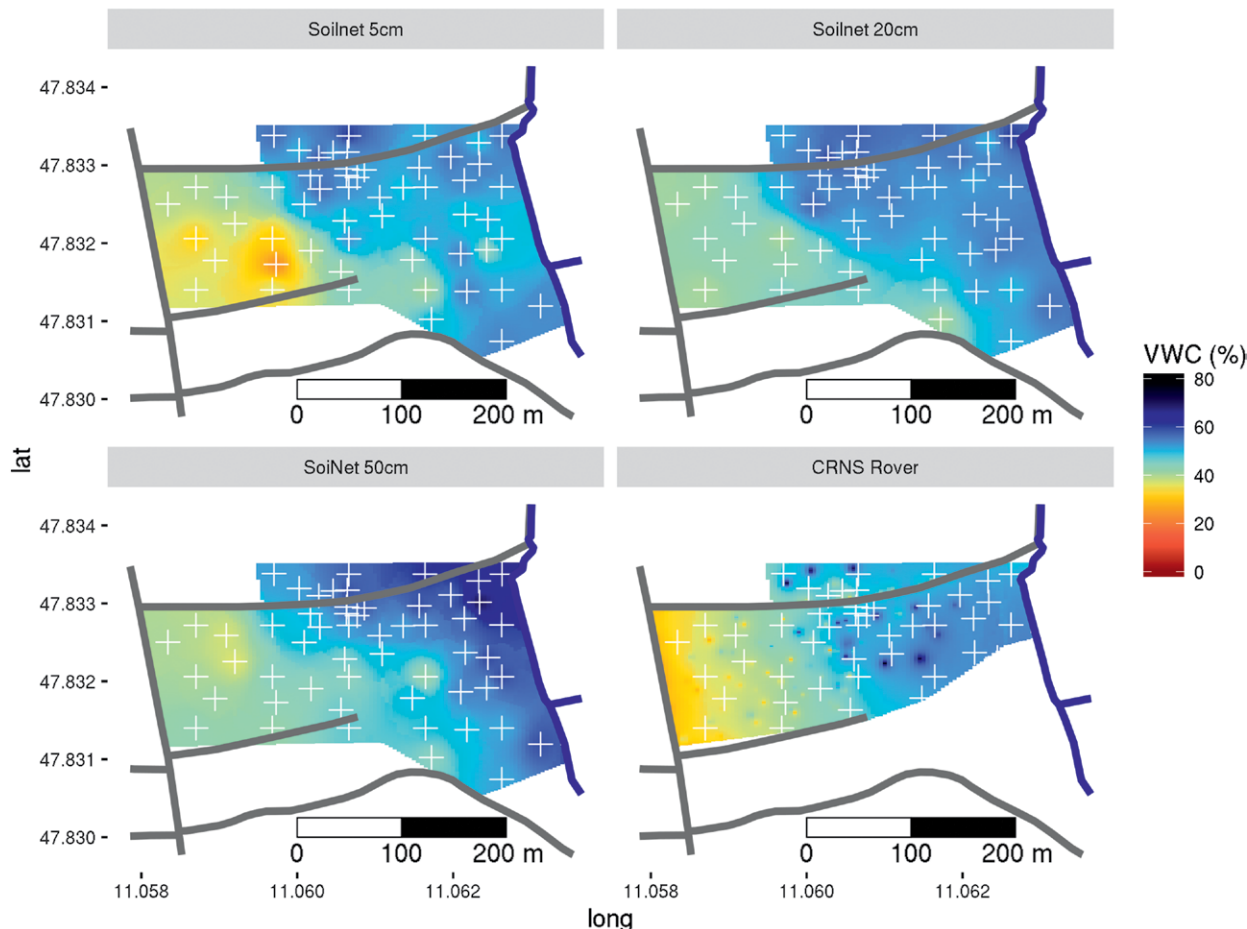
FIG. 7. Volumetric water content for 1 Jul 2015, derived from SoilNetFen at the DE-Fen site for different depths and from the CRNS Rover. Gray lines represent roads and tracks, and the Rott River is printed in blue. The SoilNetFen profiles are marked by white crosses. The southern part of the SoilNetFen area was not accessible to the Rover. The eye structures in some regions of the maps are likely artifacts from the simple distance-weighting interpolation method used.

surprisingly, hydrochemical analysis and groundwater-level measurements indicate the existence of exchanges between groundwater and surface water (not shown here). However, the detailed mechanisms of runoff generation and storage system interactions are not satisfyingly understood in this region.

To explore the runoff-generation dynamics and the connections of stream water to the local aquifer system, the water isotopic composition was analyzed during the ScaleX campaign (Table 1) by automatically drawing stream-water samples every 6 h at the outlet of the headwater catchment (Fig. 2, location D). In addition, groundwater was manually sampled biweekly in a groundwater well and batch samples of precipitation were collected weekly close to the EC station.

Figure 8 shows an overview of observed precipitation, stream discharge, groundwater-table variations, and the $\delta^{18}O$ isotopic composition of water from

these three hydrological compartments over the ScaleX-2015 period. Figure 8a demonstrates that the relatively strong rainfall events in the first half of the campaign were closely tracked by peaks in discharge. Figure 8b indicates that precipitation water tends to exhibit higher $\delta^{18}O$ values than groundwater (which varies only slightly). In contrast, the stream-water isotope signature is evidently reacting rapidly to inputs from precipitation (with its higher isotope signature). Despite different sampling frequencies, the isotopic enrichment of stream water after strong rainfall events suggests that infiltration or drainage of excess water was the dominant runoff mechanism during rainfall events. During the recession of streamflow, the contribution of groundwater to runoff increased, resulting in very similar isotopic compositions of stream water and groundwater in the low-flow period observed during the comparatively dry second half of the campaign.
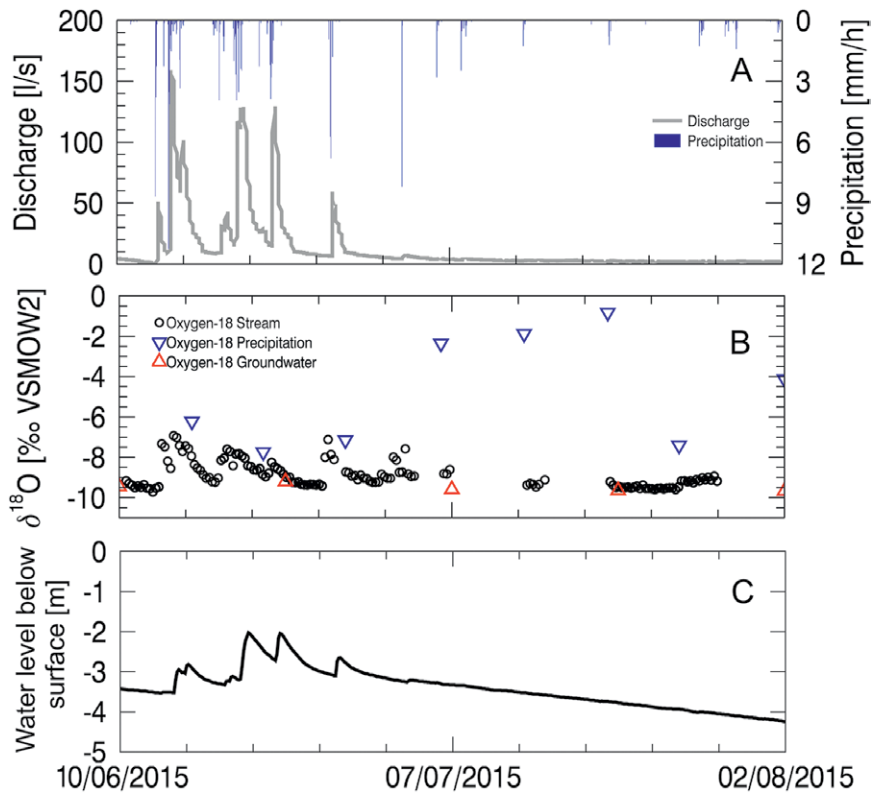
Fɪɢ. 8. (a) Rainfall intensity and stream discharge measured at the location of the automatic water sampler; (b) isotopic composition of precipitation, stream water, and groundwater; and (c) groundwater level during the ScaleX-2015 campaign. Gaps in stream-water isotopic composition were caused by instrumental failure.

The data in Fig. 8 illustrate the usefulness of continuous time series of isotopic water signatures to identify response times of flow regimes, the recharge of water storage bodies, and mixing processes. Such data, in conjunction with regional-scale hydrometeorological and soil moisture information presented above (Figs. 6 and 7), form a valuable test bed for model evaluation and as ground truth for satellite-based estimates of the land surface water balance. To this end, and to integrate local observations of soil moisture over the region, airborne and satellite remote sensing methods are used. During the 2015 campaign, an airborne synthetic aperture radar mission (F-SAR, fully polarimetric L band) was conducted by the German Aerospace Center [Deutsches Zentrum für Luft- und Raumfahrt (DLR)] over the ScaleX area, and a spaceborne SAR (*RadarSat-2*) scene was acquired for the entire the TERENO-preAlpine observatory region.

DISCUSSION AND OUTLOOK. Integrated observation programs of ecosystem–atmosphere interactions are always intensive in instrumentation and labor. To conserve costs, long-term observatory operations are commonly based on well-proven, mostly automated measurement systems, concentrated on a small number of locations. Such systems constitute the long-term backbone to building a better understanding of interactions and feedbacks between the atmosphere (from turbulence to climatic scales) and ecosystems (from photosynthesis to the life cycle of vegetation). In contrast, short-term intensive campaigns are useful for pursuing specific research goals with an all-out and focused effort. Past examples of intensive campaigns have shown them to be fertile spawning grounds for collaboration and research innovation. The ScaleX concept combines the benefits of both long-term monitoring and short-term intensive approaches. It uses an integrated TERENO long-term observatory site, with its backbone infrastructure, logistics, and long-term expertise, as the staging area for repeated short intensive campaigns. The continuity of the backbone measurements and the broad spectrum of campaign observations complement each other.

In the coming months and years, more comprehensive and interdisciplinary analyses of ScaleX-2015 data are anticipated, beyond the few examples presented here, and these will likely lead to new insights on scale interactions of ecosystem–atmosphere processes in complex terrain. In such analyses, modeling activities from single-process models to fully coupled regional climate models or large-eddy simulation systems will play important roles as scale integrators, as well as in pinpointing process interrelations and feedback mechanisms that are reflected in the data. Meanwhile, enhanced ScaleX and TERENO data products will likely serve for model performance evaluations across a wide range of scales and applications. For example, Hingerl et al. (2016) used energy balance measurements from TERENO-preAlpine

for the evaluation and analysis of the distribution of water and energy fluxes over the Rott River catchment, computed by GEOtop, a distributed water and energy balance model for complex terrain (www .geotop.org).

An important aspect of the ScaleX concept is that the same study area will be revisited by recurring campaigns. After its inception in 2015, the second ScaleX campaign, ScaleX-2016, took place in June and July 2016, and periodic further campaigns are planned throughout the lifetime of TERENO. Data from these campaigns are stored in an online ScaleX cloud that is freely available to all partners collaborating in measurements, modeling, or data mining. For access to the cloud, visit the ScaleX website (www.scalex.imk-ifu.kit .edu) or contact the corresponding author.

As we progress, we hope that ScaleX will become more integrated in terms of in situ observations, remote sensing, and modeling, and that the spectrum of observations continues to grow toward a more comprehensive modeling test bed for processes at the interface of soils, vegetation, and the atmosphere. To follow up and go beyond the specific research questions of ScaleX-2015 (see the background section above), we invite expertise on specific topics for future ScaleX campaigns, including i) the contribution of advective terms to EC flux measurements; ii) simulation of farm-animal-related emissions to derive CH_4 source strengths at catchment scale; iii) atmospheric transport modeling to link point sources to background emission, along with NBL concentration profiles of trace gases; iv) miniaturization of trace-gas sensors for UAVs; v) spaceborne and airborne remote sensing estimates of soil moisture and precipitation, land cover, elevation, and biomass productivity; and vi) advanced coupled soil–vegetation–atmosphere exchange modeling. Over time, the group of scientists and institutions that participates in ScaleX is expected to evolve, as will the topical foci, and thus this paper is an invitation to collaborate in future ScaleX campaigns and to emulate the ScaleX concept at other long-term observatory sites.

REFERENCES

Baldocchi, D., 2003: Assessing the eddy covariance technique for evaluating carbon dioxide exchange rates of ecosystems: Past, present and future. *Global Change Biol.*, **9**, 479–492, doi:10.1046/j.1365 -2486.2003.00629.x.

Beniston, M., 2006: Mountain weather and climate: A general overview and a focus on climatic change in the Alps. *Hydrobiologia*, **562**, 3–16, doi:10.1007 /s10750-005-1802-0.

Best, M. J., and Coauthors, 2015: The plumbing of land surface models: Benchmarking model performance. *J. Hydrometeor.*, **16**, 1425–1442, doi:10.1175/JHM -D-14-0158.1.

Boden, T. A., M. Krassovski, and B. Yang, 2013: The AmeriFlux data activity and data system: An evolving collection of data management techniques, tools, products and services. *Geosci. Instrum. Methods Data Syst.*, **2**, 165–176, doi:10.5194/gi-2-165-2013.

Bogena, H., 2010: Potential of wireless sensor networks for measuring soil water content variability. *Vadose Zone J.*, **9**, 1002–1013, doi:10.2136/vzj2009.0173.

Böhm, R., I. Auer, M. Brunetti, M. Maugeri, T. Nanni, and W. Schöner, 2001: Regional temperature variability in the European Alps: 1760–1998 from homogenized instrumental time series. *Int. J. Climatol.*, **21**, 1779–1801, doi:10.1002/joc.689.

Bünzli, D., and H. P. Schmid, 1998: The influence of surface texture on regionally aggregated evaporation and energy partitioning. *J. Atmos. Sci.*, **55**, 961–972, doi:10.1175/1520-0469(1998)055<0961:TIOSTO>2 .0.CO;2.

Calanca, P., 2007: Climate change and drought occurrence in the Alpine region: How severe are becoming the extremes? *Global Planet. Change*, **57**, 151–160, doi:10.1016/j.gloplacha.2006.11.001.

Caldwell, M. M., P. A. Matson, C. Wessman, and J. Gamon, 1993: Prospects for scaling. *Scaling Physiological Processes: Leaf to Globe*, J. R. Ehleringer and C. B. Field, Eds., Academic Press, 223–230.

Clark, M. P., and Coauthors, 2015: Improving the representation of hydrologic processes in Earth System Models. *Water Resour. Res.*, **51**, 5929–5956, doi:10.1002/2015WR017096.

Clough, T. J., F. M. Kelliher, R. R. Sherlock, and C. D. Ford, 2004: Lime and soil moisture effects on nitrous oxide emissions from a urine patch. *Soil Sci. Soc. Amer. J.*, **68**, 1600–1609, doi:10.2136/sssaj2004.1600.

Coplen, T., A. Herczeg, and C. Barnes, 2000: Isotope engineering—Using stable isotopes of the water molecule to solve practical problems. *Environmental Tracers in Subsurface Hydrology*, P. Cook and A. Herczeg, Eds., 79–110, doi:10.1007/978-1-4615-4557-6_3.

Denmead, O. T., M. R. Raupach, F. X. Dunin, H. A. Cleugh, and R. Leuning, 1996: Boundary layer budgets for regional estimates of scalar fluxes. *Global Change Biol.*, **2**, 255–264, doi:10.1111/j.1365-2486.1996.tb00077.x.

Desai, A. R., and Coauthors, 2011: Seasonal pattern of regional carbon balance in the central Rocky Mountains from surface and airborne measurements. *J. Geophys. Res.*, **116**, G04009, doi:10.1029/2011JG001655.

Ehleringer, J. R., and C. B. Field, Eds., 1993: *Scaling Physiological Processes: Leaf to Globe*. Academic Press, 388 pp.

Emeis, S., 2008: Examples for the determination of turbulent (sub-synoptic) fluxes with inverse methods. *Meteor. Z.*, **17**, 3–11, doi:10.1127/0941-2948/2008/0265.

——, 2015: Observational techniques to assist the coupling of CWE/CFD models and meso-scale meteorological models. *J. Wind Eng. Ind. Aerodyn.*, **144**, 24–30, doi:10.1016/j.jweia.2015.04.018.

——, K. Schäfer, and C. Münkel, 2009: Observation of the structure of the urban boundary layer with different ceilometers and validation by RASS data. *Meteor. Z.*, **18**, 149–154, doi:10.1127/0941-2948/2009/0365.

Finnigan, J. J., 2004: The footprint concept in complex terrain. *Agric. For. Meteor.*, **127**, 117–129, doi:10.1016/j.agrformet.2004.07.008.

Firestein, S., 2012: *Ignorance: How It Drives Science*. Oxford University Press, 208 pp.

Goring, S. J., and Coauthors, 2014: Improving the culture of interdisciplinary collaboration in ecology by expanding measures of success. *Front. Ecol. Environ.*, **12**, 39–47, doi:10.1890/120370.

Hall, F. G., 1999: Introduction to special section: BOREAS in 1999: Experiment and science overview. *J. Geophys. Res.*, **104**, 27 627–27 639, doi:10.1029/1999JD901026.

Hingerl, L., H. Kunstmann, S. Wagner, M. Mauder, J. Bliefernicht, and R. Rigon, 2016: Spatiotemporal variability of water and energy fluxes—A case study for a mesoscale catchment in pre-alpine environment. *Hydrol. Processes*, **30**, 3804–3823, doi:10.1002/hyp.10893.

Hinkle, S. R., J. H. Duff, F. J. Triska, A. Laenen, E. B. Gates, K. E. Bencala, D. A. Wentz, and S. R. Silva, 2001: Linking hyporheic flow and nitrogen cycling near the Willamette River—A large river in Oregon, USA. *J. Hydrol.*, **244**, 157–180, doi:10.1016/S0022-1694(01)00335-3.

Hommeltenberg, J., M. Mauder, M. Drösler, K. Heidbach, P. Werle, and H. P. Schmid, 2014: Ecosystem scale methane fluxes in a natural temperate bog-pine forest in southern Germany. *Agric. For. Meteor.*, **198–199**, 273–284, doi:10.1016/j.agrformet.2014.08.017.

Jones, J. B., and R. M. Holmes, 1996: Surface–subsurface interactions in stream ecosystems. *Trends Ecol. Evol.*, **11**, 239–242, doi:10.1016/0169-5347(96)10013-6.

Junkermann, W., 2001: An ultralight aircraft as platform for research in the lower troposphere: System performance and first results from radiation transfer studies in stratiform aerosol layers and broken cloud conditions. *J. Atmos. Oceanic Technol.*, **18**, 934–946, doi:10.1175/1520-0426(2001)018<0934:AUAAPF>2.0.CO;2.

——, R. Hagemann, and B. Vogel, 2011: Nucleation in the Karlsruhe plume during the COPS/TRACKS-Lagrange experiment. *Quart. J. Roy. Meteor. Soc.*, **137**, 267–274, doi:10.1002/qj.753.

Kalbus, E., F. Reinstorf, and M. Schirmer, 2006: Measuring methods for groundwater–surface water interactions: A review. *Hydrol. Earth Syst. Sci.*, **10**, 873–887, doi:10.5194/hess-10-873-2006.

Kampe, T., B. R. Johnson, M. Kuester, and M. Keller, 2010: NEON: The first continental-scale ecological observatory with airborne remote sensing of vegetation canopy biochemistry and structure. *J. Appl. Remote Sens.*, **4**, 043510, doi:10.1117/1.3361375.

Köhli, M., M. Schrön, M. Zreda, U. Schmidt, P. Dietrich, and S. Zacharias, 2015: Footprint characteristics revised for field-scale soil moisture monitoring with cosmic-ray neutrons. *Water Resour. Res.*, **51**, 5772–5790, doi:10.1002/2015WR017169.

Krajewski, W. F., G. J. Ciach, and E. Habib, 2003: An analysis of small-scale rainfall variability in different climatic regimes. *Hydrol. Sci. J.*, **48**, 151–162, doi:10.1623/hysj.48.2.151.44694.

Levin, S. A., 1992: The problem of pattern and scale in ecology. *Ecology*, **73**, 1943–1967, doi:10.2307/1941447.

Lorenz, C., and H. Kunstmann, 2012: The hydrological cycle in three state-of-the-art reanalyses:

Intercomparison and performance analysis. *J. Hydrometeor.*, **13**, 1397–1420, doi:10.1175/JHM-D-11-088.1.

Mahrt, L., 1987: Grid-averaged surface fluxes. *Mon. Wea. Rev.*, **115**, 1550–1560, doi:10.1175/1520-0493 (1987)115<1550:GASF>2.0.CO;2.

——, 2010: Computing turbulent fluxes near the surface: Needed improvements. *Agric. For. Meteor.*, **150**, 501–509, doi:10.1016/j.agrformet.2010.01.015.

Mauder, M., R. L. Desjardins, E. Pattey, and D. Worth, 2010: An attempt to close the daytime surface energy balance using spatially-averaged flux measurements. *Bound.-Layer Meteor.*, **136**, 175–191, doi:10.1007 /s10546-010-9497-9.

——, M. Cuntz, C. Drüe, A. Graf, C. Rebmann, H. P. Schmid, M. Schmidt, and R. Steinbrecher, 2013: A strategy for quality and uncertainty assessment of long-term eddy-covariance measurements. *Agric. For. Meteor.*, **169**, 122–135, doi:10.1016/j. agrformet.2012.09.006.

May, R., 1999: Unanswered questions in ecology. *Philos. Trans. Roy. Soc. London*, **354B**, 1951–1959, doi:10.1098/rstb.1999.0534.

Metzger, S., and Coauthors, 2013: Spatially explicit regionalization of airborne flux measurements using environmental response functions. *Biogeosciences*, **10**, 2193–2217, doi:10.5194/bg-10-2193-2013.

Mills, R. T. E., K. S. Gavazov, T. Spiegelberger, D. Johnson, and A. Buttler, 2014: Diminished soil functions occur under simulated climate change in a sup-alpine pasture, but heterotrophic temperature sensitivity indicates microbial resilience. *Sci. Total Environ.*, **473–474**, 465–472, doi:10.1016/j.scitotenv.2013.12.071.

Orlanski, I., 1975: A rational subdivision of scales for atmospheric processes. *Bull. Amer. Meteor. Soc.*, **56**, 527–530.

Osmond, B., and Coauthors, 2004: Changing the way we think about global change research: Scaling up in experimental ecosystem science. *Global Change Biol.*, **10**, 393–407, doi:10.1111/j.1529-8817.2003.00747.x.

Pebesma, E. J., 2004: Multivariable geostatistics in S: The gstat package. *Comput. Geosci.*, **30**, 683–691, doi:10.1016/j.cageo.2004.03.012.

Pihlatie, M. K., and Coauthors, 2010: Greenhouse gas fluxes in a drained peatland forest during spring frost-thaw event. *Biogeosciences*, **7**, 1715–1727, doi:10.5194/bg-7-1715-2010.

——, and Coauthors, 2013: Comparison of static chambers to measure CH_4 emissions from soils. *Agric. For. Meteor.*, **171–172**, 124–136, doi:10.1016/j .agrformet.2012.11.008.

Poulos, M. J., J. L. Pierce, A. N. Flores, and S. G. Benner, 2012: Hillslope asymmetry maps reveal widespread, multi-scale organization. *Geophys. Res. Lett.*, **39**, L06406, doi:10.1029/2012GL051283.

Reid, W. V., and Coauthors, 2005: *Millenium Ecosystem Assessment: Ecosystems and Well-Being: Synthesis.* Island Press, 155 pp. [Available online at www .millenniumassessment.org/documents/document .356.aspx.pdf.]

Ruehr, N. K., B. E. Law, D. Quandt, and M. Williams, 2014: Effects of heat and drought on carbon and water dynamics in a regenerating semi-arid pine forest: A combined experimental and modeling approach. *Biogeosciences*, **11**, 4139–4156, doi:10.5194 /bg-11-4139-2014.

Schäfer, K., J. Böttcher, D. Weymann, C. von der Heide, and W. H. M. Duijnisveld, 2012: Evaluation of a closed tunnel for field-scale measurements of nitrous oxide fluxes from an unfertilized grassland soil. *J. Environ. Qual.*, **41**, 1383, doi:10.2134 /jeq2011.0475.

Schmid, H. P., 2002: Footprint modeling for vegetation atmosphere exchange studies: A review and perspective. *Agric. For. Meteor.*, **113**, 159–183, doi:10.1016 /S0168-1923(02)00107-7.

——, and C. R. Lloyd, 1999: Spatial representativeness and the location bias of flux footprints over inhomogeneous areas. *Agric. For. Meteor.*, **93**, 195–209, doi:10.1016/S0168-1923(98)00119-1.

Sellers, P. J., F. G. Hall, G. Asrar, D. E. Strebel, and R. E. Murphy, 1988: The First ISLSCP Field Experiment (FIFE). *Bull. Amer. Meteor. Soc.*, **69**, 22–27, doi:10.1175/1520-0477(1988)069<0022:TFIFE >2.0.CO;2.

——, F. G. Hall, G. Asrar, D. E. Strebel, and R. E. Murphy, 1992: An overview of the First International Satellite Land Surface Climatology Project (ISLSCP) Field Experiment (FIFE). *J. Geophys. Res.*, **97**, 18 345– 18 371, doi:10.1029/92JD02111.

——, and Coauthors, 1995: The Boreal Ecosystem– Atmosphere Study (BOREAS): An overview and early results from the 1994 field year. *Bull. Amer. Meteor. Soc.*, **76**, 1549–1577, doi:10.1175/1520-0477 (1995)076<1549:TBESAO>2.0.CO;2.

Smiatek, G., H. Kunstmann, R. Knoche, and A. Marx, 2009: Precipitation and temperature statistics in high-resolution regional climate models: Evaluation for the European Alps. *J. Geophys. Res.*, **114**, D19107, doi:10.1029/2008JD011353.

Sophocleous, M., 2002: Interactions between groundwater and surface water: The state of the science. *Hydrogeol. J.*, **10**, 52–67, doi:10.1007/s10040-001-0170-8.

Stoy, P. C., and Coauthors, 2013: A data-driven analysis of energy balance closure across FLUXNET research sites: The role of landscape scale heterogeneity.

Agric. For. Meteor., **171–172**, 137–152, doi:10.1016/j.agrformet.2012.11.004.

Sun, J., and Coauthors, 2010: A multiscale and multidisciplinary investigation of ecosystem–atmosphere CO_2 exchange over the Rocky Mountains of Colorado. *Bull. Amer. Meteor. Soc.*, **91**, 209–230, doi:10.1175/2009BAMS2733.1.

Tetzlaff, D., J. Seibert, K. J. McGuire, H. Laudon, D. A. Burns, S. M. Dunn, and C. Soulsby, 2009: How does landscape structure influence catchment transit time across different geomorphic provinces. *Hydrol. Processes*, **23**, 945–953, doi:10.1002/hyp.7240.

Uhlenbrook, S., M. Frey, C. Leibundgut, and P. Maloszewski, 2002: Hydrograph separations in a mesoscale mountainous basin at event and seasonal timescales. *Water Resour. Res.*, **38**, doi:10.1029/2001WR000938.

Yao, Z., X. Wu, B. Wolf, M. Dannenmann, K. Butterbach-Bahl, N. Brueggemann, W. W. Chen, and X. H. Zheng, 2010: Soil-atmosphere exchange potential of NO and N_2O in different land use types of Inner Mongolia as affected by soil temperature, soil moisture, freeze-thaw, and drying-wetting events. *J. Geophys. Res.*, **115**, D17116, doi:10.1029/2009JD013528.

Zacharias, S., and Coauthors, 2011: A network of terrestrial environmental observatories in Germany. *Vadose Zone J.*, **10**, 955, doi:10.2136/vzj2010.0139.

Zeeman, M. J., M. Mauder, R. Steinbrecher, K. Heidbach, E. Eckart, and H. P. Schmid, 2017: Reduced snow cover affects productivity of upland temperate grasslands. *Agric. For. Meteor.*, **232**, 514–526, doi:10.1016/j.agrformet.2016.09.002.

Zreda, M., D. Desilets, T. P. A. Ferre, and R. L. Scott, 2008: Measuring soil moisture content non-invasively at intermediate spatial scale using cosmic-ray neutrons. *Geophys. Res. Lett.*, **35**, L21402, doi:10.1029/2008GL035655.